



## Experimental Evidence for Two Gaps in the High-Temperature La<sub>1.83</sub>Sr<sub>0.17</sub>CuO<sub>4</sub> Superconductor

R. Khasanov,<sup>1</sup> A. Shengelaya,<sup>2</sup> A. Maisuradze,<sup>1</sup> F. La Mattina,<sup>1</sup> A. Bussmann-Holder,<sup>3</sup> H. Keller,<sup>1</sup> and K. A. Müller<sup>1</sup>

<sup>1</sup>Physik-Institut der Universität Zürich, Winterthurerstrasse 190, CH-8057 Zürich, Switzerland

<sup>2</sup>Physics Institute of Tbilisi State University, Chavchavadze 3, GE-0128 Tbilisi, Georgia

<sup>3</sup>Max-Planck-Institut für Festkörperforschung, Heisenbergstrasse 1, D-70569 Stuttgart, Germany

(Received 7 June 2006; published 2 February 2007)

The in-plane magnetic field penetration depth ( $\lambda_{ab}$ ) in single-crystal La<sub>1.83</sub>Sr<sub>0.17</sub>CuO<sub>4</sub> was investigated by muon-spin rotation ( $\mu$ SR). The temperature dependence of  $\lambda_{ab}^{-2}$  has an inflection point around 10–15 K, suggesting the presence of two superconducting gaps: a large gap ( $\Delta_1^d$ ) with  $d$ -wave and a small gap ( $\Delta_2^s$ ) with  $s$ -wave symmetry. The zero-temperature values of the gaps at  $\mu_0 H = 0.02$  T were found to be  $\Delta_1^d(0) = 8.2(1)$  meV and  $\Delta_2^s(0) = 1.57(8)$  meV.

DOI: 10.1103/PhysRevLett.98.057007

PACS numbers: 74.72.Dn, 74.25.Ha, 76.75.+i

It is mostly believed that the order parameter in cuprate high-temperature superconductors (HTS) has purely  $d$ -wave symmetry, as indicated by, e.g., tricrystal experiments [1]. There are, however, a wide variety of experimental data that support  $s$  or even more complicated types of symmetries ( $d + s$ ,  $d + is$ , etc.) [2]. In order to solve this controversy, Müller suggested the presence of two superconducting condensates with different symmetries ( $s$ - and  $d$ -wave) in HTS [3,4]. This idea was generated partly because two gaps were observed in  $n$ -type SrTiO<sub>3</sub> [5], the first oxide in which superconductivity was detected. In addition, it is known that the two-order parameter scenario leads to a substantial enhancement of the superconducting transition temperature in comparison to a single-band model [6,7]. The two-band model was successfully used to explain superconductivity in MgB<sub>2</sub> [8] and is considered also to be relevant to understand superconductivity in HTS [7,9].

Important information on the symmetry of the order parameter can be obtained from magnetic field penetration depth ( $\lambda$ ) measurements. In particular,  $\lambda(T)$ , which reflects the quasiparticle density of states available for thermal excitations, admits to probe the superconducting gap structure. Measurements of the field dependence of  $\lambda$  allow the study of the anisotropy of the superconducting energy gap [10] and, in the case of two-gap superconductors, to obtain details on the relative contribution of each particular gap as a function of magnetic field [11]. In this Letter we report a study of the in-plane magnetic penetration depth ( $\lambda_{ab}$ ) in slightly overdoped single-crystal La<sub>1.83</sub>Sr<sub>0.17</sub>CuO<sub>4</sub> by muon-spin-rotation ( $\mu$ SR). At low magnetic fields ( $\mu_0 H \lesssim 0.3$  T)  $\lambda_{ab}^{-2}(T)$  exhibits an inflection point at  $T \approx 10$ –15 K. We interpret this feature as a consequence of the presence of two superconducting gaps. It is suggested that the large gap [ $\Delta_1^d(0) = 8.2(1)$  meV] has  $d$ - and the small gap [ $\Delta_2^s(0) = 1.57(8)$  meV]  $s$ -wave symmetry. With increasing magnetic field, the contribution of  $\Delta_2^s$  decreases substantially, in contrast to an almost constant contribution of  $\Delta_1^d$ . Both the temperature and the field dependences of

$\lambda_{ab}^{-2}$  were found to be similar to what was observed in double-gap MgB<sub>2</sub> [11,12].

The La<sub>1.83</sub>Sr<sub>0.17</sub>CuO<sub>4</sub> single crystal was grown by the traveling solvent floating zone technique [13]. The transition temperature  $T_c$  and the width of the superconducting transition at  $\mu_0 H \approx 0$  T were found to be 36.2 and 1.5 K, respectively [14]. The  $\mu$ SR experiments were performed at the  $\pi$ M3 beam line at the Paul Scherrer Institute (Villigen, Switzerland). Typical counting statistics were  $\sim 16$ –18 million muon detections over three detectors. The sample was field cooled from above  $T_c$  to 1.6 K in a series of fields ranging from 20 mT to 0.64 T. The sample was aligned such that the  $c$  axis was parallel (within 1°, as measured by Laue x-ray diffraction) to the external magnetic field. In the transverse-field geometry, the local magnetic field distribution  $P(B)$  probed by  $\mu$ SR inside the superconducting sample in the mixed state is determined by the coherence length  $\xi$  and the penetration depth  $\lambda$ . In extreme type II superconductors ( $\lambda \gg \xi$ )  $P(B)$  is almost independent of  $\xi$ , and the second moment of  $P(B)$  is proportional to  $1/\lambda^4$  [15].

Figure 1 shows the magnetic field distributions  $P(B)$  for single-crystal La<sub>1.83</sub>Sr<sub>0.17</sub>CuO<sub>4</sub> at  $T = 1.7$  K obtained by means of the maximum entropy Fourier transform technique. In order to extract the second moment of  $P(B)$  we used a similar procedure as described in Ref. [16]. All  $\mu$ SR time spectra were fitted by a three component expression:

$$P(t) = \sum_{i=1}^3 A_i \exp(-\sigma_i^2 t^2 / 2) \cos(\gamma_\mu B_i t + \phi). \quad (1)$$

Here  $A_i$ ,  $\sigma_i$ , and  $B_i$  are the asymmetry, the relaxation rate, and the mean field of the  $i$ th component, and  $\phi$  is the initial phase of the muon-spin ensemble. The first and the second moments of  $P(B)$  are [16]

$$\langle B \rangle = \sum_{i=1}^3 \frac{A_i B_i}{A_1 + A_2 + A_3} \quad (2)$$

and

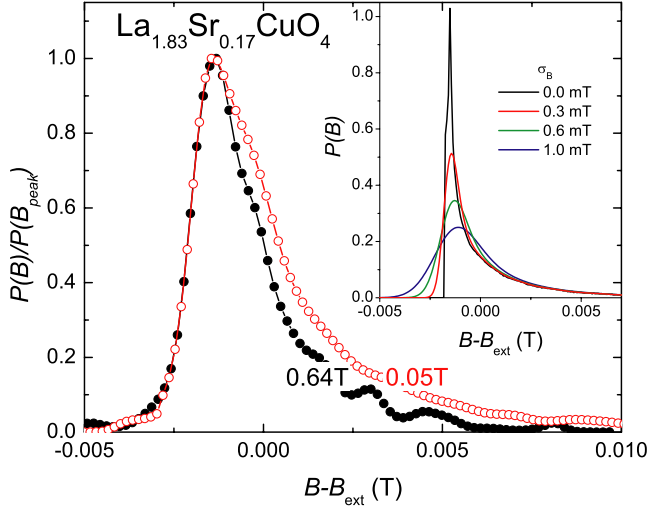


FIG. 1 (color online). Local magnetic field distribution  $P(B)$  in the mixed state of single-crystal  $\text{La}_{1.83}\text{Sr}_{0.17}\text{CuO}_4$  ( $T = 1.7$  K, field cooled) normalized to their maximum value at  $B = B_{\text{peak}}$  for 0.05 and 0.64 T. The inset shows theoretical  $P(B)$  distributions ( $\lambda = 220$  nm,  $\xi = 2$  nm, and  $\mu_0 H = 0.05$  T) for different values of the smearing parameter  $\sigma_B = 0, 0.3, 0.6,$  and  $1.0$  mT.

$$\langle \Delta B^2 \rangle = \frac{\sigma^2}{\gamma_\mu^2} = \sum_{i=1}^3 \frac{A_i}{A_1 + A_2 + A_3} \{ (\sigma_i / \gamma_\mu)^2 + [B_i - \langle B \rangle]^2 \}, \quad (3)$$

where  $\gamma_\mu = 2\pi \times 135.5342$  MHz/T is the muon gyromagnetic ratio. The superconducting part of the square root of the second moment ( $\sigma_{\text{sc}} \propto \lambda_{\text{ab}}^{-2}$ ) was then obtained by subtracting the nuclear moment contribution ( $\sigma_{\text{nm}}$ ) measured at  $T > T_c$  according to  $\sigma_{\text{sc}}^2 = \sigma^2 - \sigma_{\text{nm}}^2$  [16]. To ensure that the increase of  $\sigma$  below  $T_c$  is attributed entirely to the vortex lattice, zero-field  $\mu\text{SR}$  experiments were performed. The experiments show no evidence for static magnetism in  $\text{La}_{1.83}\text{Sr}_{0.17}\text{CuO}_4$  down to 1.7 K.

In Fig. 2 we plot the temperature dependences of  $\sigma_{\text{sc}} \propto \lambda_{\text{ab}}^{-2}$  for  $\mu_0 H = 0.02, 0.1,$  and  $0.64$  T (for clarity, data for 0.05 and 0.3 T are not shown). Most importantly, around 10–15 K an inflection point appears. It is well pronounced at  $\mu_0 H = 0.02$  T and almost absent at  $\mu_0 H = 0.64$  T. In Ref. [17] it was pointed out that an inflection point in  $\lambda^{-2}(T)$  may appear in superconductors with two weakly coupled superconducting bands. Indeed, in  $\text{MgB}_2$ , where the  $\sigma$ - and  $\pi$ -bands are almost decoupled, an upward curvature of  $\lambda^{-2}(T)$ , similar to the one observed for  $\text{La}_{1.83}\text{Sr}_{0.17}\text{CuO}_4$  at  $\mu_0 H = 0.02$  T (Fig. 2), was detected (see, e.g., [12]). Thus, in analogy to  $\text{MgB}_2$ , we analyze our data by assuming that  $\sigma_{\text{sc}}$  is a linear combination of two terms [18,19]:

$$\sigma_{\text{sc}}(T)/\sigma_{\text{sc}}(0) = \omega \delta\sigma[\Delta_1(0), T] + (1 - \omega) \delta\sigma[\Delta_2(0), T]. \quad (4)$$

Here  $\Delta_1(0)$  and  $\Delta_2(0)$  are the zero-temperature values of the large and the small gap, respectively, and  $\omega$  ( $0 \leq \omega \leq$

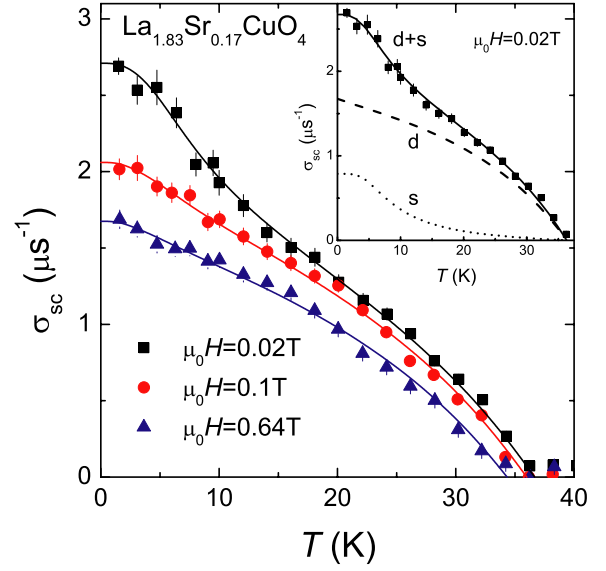


FIG. 2 (color online). Temperature dependence of  $\sigma_{\text{sc}} \propto \lambda_{\text{ab}}^{-2}$  of single-crystal  $\text{La}_{1.83}\text{Sr}_{0.17}\text{CuO}_4$  measured at 0.02, 0.1, and 0.64 T (field cooled). Lines in the main figure and in the inset represent the fit with the two-gap model [Eq. (4)]. In the inset the contributions from the large  $d$ -wave gap and the small  $s$ -wave gap entering Eq. (4) are shown separately. See text for details.

1) is the weighting factor which measures their relative contributions to  $\lambda^{-2}$ . Note, that in contrast to  $\text{MgB}_2$ , where both gaps are isotropic, in HTS at least one gap has  $d$ -wave symmetry [1]. Concerning the symmetry of the second gap, however, the situation is unclear. Based on the observation of a substantial  $s$ -wave contribution to the superconducting order parameter by Andreev reflection experiments [2] and on the analysis of tunneling data [3], we assume that the second gap has isotropic  $s$ -wave symmetry. Thus, for the contribution to  $\sigma_{\text{sc}}$  arising from the  $s$ -wave gap, we used the standard relation [19]

$$\delta\sigma[T, \Delta^s(0)] = 1 + 2 \int_{\Delta^s(T)}^{\infty} \left( \frac{\partial f}{\partial E} \right) \frac{E}{\sqrt{E^2 - \Delta^s(T)^2}} dE. \quad (5)$$

Here  $f = [1 + \exp(E/k_B T)]^{-1}$  is the Fermi function,  $k_B$  is the Boltzmann constant, and  $\Delta^s(T) = \Delta^s(0) \tilde{\Delta}^s(T/T_c)$  represents the temperature dependence of the  $s$ -wave gap with the tabulated gap values  $\tilde{\Delta}^s(T/T_c)$  from [20]. For the  $d$ -wave gap contribution we take  $\Delta^d(T, \varphi) = \Delta^s(T) \times \cos(2\varphi)$  [2] and

$$\delta\sigma[T, \Delta^d(0)] = 1 + 1/\pi \int_0^{2\pi} \int_{\Delta^d(T, \varphi)}^{\infty} \left( \frac{\partial f}{\partial E} \right) \times \frac{E}{\sqrt{E^2 - \Delta^d(T, \varphi)^2}} dE d\varphi. \quad (6)$$

In order to determine the symmetry of the two gaps, the field-cooled 0.05 T data were analyzed within “ $d + s$ ” and “ $s + d$ ” scenarios using Eq. (4). The analysis reveals for  $d + s$ :  $\Delta_1^d(0) = 9.0(2)$  meV,  $\Delta_2^s(0) = 1.7(1)$  meV,  $\omega = 0.69(3)$ , and for  $s + d$ :  $\Delta_1^s(0) = 6.2(2)$  meV,

TABLE I. Summary of the two-gap analysis for single-crystal  $\text{La}_{1.83}\text{Sr}_{0.17}\text{CuO}_4$ . The meaning of the parameters is explained in the text.

$\mu_0 H$ (T)	$T_c$ (K)	$\sigma_{sc}(0)$ ( $\mu\text{s}^{-1}$ )	$\omega$	$\Delta_1^d(0)$ (meV)	$\Delta_2^s(0)$ (meV)	$\frac{2\Delta_1^d(0)}{k_B T_c}$	$\frac{2\Delta_2^s(0)}{k_B T_c}$
0.02	36.3(1)	2.71(8)	0.68(3)	8.2(1)	1.57(8)		
0.05	36.1(1)	2.20(7)	0.78(2)	8.2(1)	1.56(8)		
0.1	35.5(1)	2.07(7)	0.88(2)	8.0(1)	1.54(8)	5.24(7) <sup>a</sup>	1.00(5) <sup>a</sup>
0.3	34.7(1)	1.82(6)	0.92(2)	7.8(1)	1.50(7)		
0.64	34.0(1)	1.71(5)	0.94(2)	7.7(1)	1.47(7)		

<sup>a</sup>Common fit parameter for all fields.

$\Delta_2^d(0) = 2.0(2)$  meV,  $\omega = 0.73(2)$ . Comparison with  $\Delta(0) \approx 10$  meV obtained on a similar sample by tunneling experiments [21], suggests that the large gap has  $d$ -wave symmetry. Another argument in favor of a “large”  $d$ -wave gap comes from the observation of a square vortex lattice in the same crystal as used in this work in fields higher than 0.4 T [14,22], where, as shown below, the contribution from the large gap to  $\sigma_{sc}$  is dominant. A square vortex lattice is typical for  $d$ -wave superconductors [14].

The solid lines in Fig. 2 represent the global fit of Eq. (4) to the data with contributions from the large and the small gaps described by Eqs. (5) and (6), respectively. In the analysis all the  $\sigma_{sc}(T)$  curves (0.02, 0.05, 0.1, 0.3, 0.64 T) were fitted simultaneously with  $\sigma_{sc}(0)$ ,  $T_c$ , and  $\omega$  as individual parameters for each particular data set.  $\Delta_1^d(0)$  and  $\Delta_2^s(0)$  were assumed to scale linearly with  $T_c$  according to the relation  $2\Delta(0)/k_B T_c = \text{const}$ . The results are summarized in Table I and Fig. 3. It is seen in Fig. 3(a) that the decrease of  $\sigma_{sc}(0)$  is associated with an increase of the contribution of the large gap to  $\lambda^{-2}$ . Similar field dependences of  $\omega$  and  $\sigma_{sc}$  were observed in  $\text{MgB}_2$  [11,23,24] and explained by the fact that superconductivity within the weaker  $\pi$ -band is suppressed at much lower fields than that within the stronger  $\sigma$ -band [24]. As shown in Fig. 3(b) this is also the case for  $\text{La}_{1.83}\text{Sr}_{0.17}\text{CuO}_4$ . Indeed, while the contribution from the large gap [ $\sigma_1(0) = \omega\sigma_{sc}(0)$ ] changes only slightly, the contribution from the small gap [ $\sigma_2(0) = (1 - \omega)\sigma_{sc}(0)$ ] decreases by almost an order of magnitude in the field range  $0 < \mu_0 H \leq 0.64$  T [Fig. 3(b)]. Thus, the temperature and the field dependences of  $\lambda_{ab}^{-2}$  in  $\text{La}_{1.83}\text{Sr}_{0.17}\text{CuO}_4$  are similar to  $\text{MgB}_2$ , and, consequently, demonstrate the existence of two gaps. This is the most obvious scenario, even though other gap dependences cannot be fully ruled out. Note that, the nuclear magnetic resonance [25] and the inelastic neutron scattering data [26] support this finding.

It is important to emphasize that the observation of an inflection point in  $\lambda^{-2}(T)$  is not restricted to  $\text{MgB}_2$  and the particular sample used in this work. Indication of an inflection point in  $\lambda^{-2}(T)$  was also observed in hole-doped  $\text{YBa}_2\text{Cu}_3\text{O}_{7-\delta}$  [10,27],  $\text{YBa}_2\text{Cu}_4\text{O}_8$  [28], and  $\text{La}_{1.85}\text{Sr}_{0.15}\text{CuO}_4$  [29], as well as in electron-doped  $\text{Pr}_{1.855}\text{Ce}_{0.145}\text{CuO}_{4y}$  [30]. In Ref. [27] the increase of the second moment of  $P(B)$  observed in  $\text{YBa}_2\text{Cu}_3\text{O}_{7-\delta}$  at low temperatures was attributed to pinning effects. In order to

investigate the role of pinning in our sample we compare the  $P(B)$  distributions for 0.05 and 0.64 T (Fig. 1) with theoretical  $P(B)$  curves. A standard way to account for pinning is to convolute the theoretical  $P(B)$  for an ideal vortex lattice (black line in the inset of Fig. 1) with a Gaussian distribution of fields [31]:

$$P(B) = \frac{1}{\sqrt{2\pi}\sigma_B} \int \exp\left[-\frac{1}{2}\left(\frac{B-B'}{\sigma_B}\right)^2\right] P_{id}(B') dB', \quad (7)$$

where  $\sigma_B$  is the width of the Gaussian distribution and  $P_{id}(B)$  is the field distribution for an ideal vortex lattice [10]. For a stiff vortex lattice this convolution reflects how random disorder and distortions due to flux line pinning influence the ideal  $P_{id}(B)$  [31]. The theoretical  $P(B)$  profiles for  $\sigma_B = 0, 0.3, 0.6$ , and 1.0 mT are shown in the inset of Fig. 1. The direct comparison of the  $P(B)$  data for  $\mu_0 H = 0.05$  T and 0.64 T with theoretical  $P(B)$  profiles clearly demonstrates that pinning is not the source of the increase of the second moment of  $P(B)$  at low temperatures. Indeed, pinning leads to an almost symmetric (around  $B_{\text{peak}}$ ) broadening of  $P(B)$  (see inset of Fig. 1),

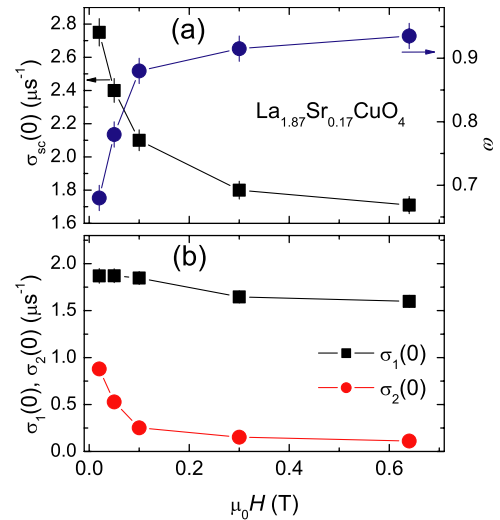


FIG. 3 (color online). (a) Field dependences of  $\sigma_{sc}(0)$  and  $\omega$  for single-crystal  $\text{La}_{1.83}\text{Sr}_{0.17}\text{CuO}_4$  obtained from the fit of Eq. (4) to the data (see Table I). (b) Contribution from the large [ $\sigma_1(0)$ ] and the small [ $\sigma_2(0)$ ] superconducting gap to the total  $\sigma_{sc}(0)$ .

while the experimental  $P(B)$  profiles very well coincide at low fields ( $B < B_{\text{peak}}$ ). Deviations only occur in the high-field tail of  $P(B)$  ( $B > B_{\text{peak}}$ ).

The obvious question which arises is where to locate the second superconducting gap in  $\text{La}_{2-x}\text{Sr}_x\text{CuO}_4$ . The phase diagram of cuprates is usually interpreted in terms of holes doped into the planar  $\text{Cu}d_{x^2-y^2}\text{-O}p_\alpha$  ( $\alpha = x, y$ ) antibonding band. In  $\text{La}_{2-x}\text{Sr}_x\text{CuO}_4$  it is assumed that one hole per Sr atom enters this band. However, recent *ab initio* calculations yielded additional features appearing on doping of  $\text{La}_{2-x}\text{Sr}_x\text{CuO}_4$  [32]. According to these calculations part of the holes occupy the  $\text{Cu}d_{3z^2-r^2}\text{-O}p_z$  orbitals. These results are supported by neutron diffraction data [33], showing that the doped holes appear in both the planar and the out-of-plane bands. In contrast to this finding, in angle-resolved photoemission (ARPES) experiments on HTS only the planar band was observed, suggesting a quasi-two-dimensional electronic structure with negligible *inter-cell* coupling of  $\text{CuO}_2$  layers (see, e.g., [34]). This is, however, inconsistent with in-plane and out-of-plane  $\lambda$  measurements [35], optical conductivity [36], and anisotropy parameter studies [37]. All these experiments demonstrate that with increasing doping cuprates become more and more three dimensional. Recently a 3D Fermi surface was observed in overdoped  $\text{TlBa}_2\text{CuO}_{6+\delta}$  [38]. Also, a careful analysis of ARPES data reveals that the finite dispersion of the energy bands along the  $z$  direction of the Brillouin zone ( $k_z$  dispersion) naturally induces an irreducible linewidth of the ARPES peaks which is unrelated to any scattering mechanism [39] and implies that out-of-plane hybridized bands have to be incorporated.

In conclusion, we performed systematic  $\mu\text{SR}$  studies of the in-plane magnetic penetration depth  $\lambda_{\text{ab}}$  in single-crystal  $\text{La}_{1.83}\text{Sr}_{0.17}\text{CuO}_4$ . Both, the magnetic field and the temperature dependences of  $\lambda_{\text{ab}}^{-2}$  were found to be consistent with the presence of two gaps. The experimental data were analyzed by assuming that the large gap ( $\Delta_1^d$ ) has *d*-wave and the small gap ( $\Delta_2^s$ ) *s*-wave symmetry. Further  $\mu\text{SR}$  investigation of the penetration depth in  $\text{La}_{2-x}\text{Sr}_x\text{CuO}_4$  at various doping levels are in progress.

This work was partly performed at the Swiss Muon Source ( $\text{S}\mu\text{S}$ ), Paul Scherrer Institute (PSI, Switzerland). The authors are grateful to N. Momono, M. Oda, M. Ido, and J. Mesot for providing us the  $\text{La}_{1.83}\text{Sr}_{0.17}\text{CuO}_4$  single crystal, J. Mesot for helpful discussions, and A. Amato, D. Herlach, and C. J. Juul for assistance during the  $\mu\text{SR}$  measurements. This work was supported by the Swiss National Science Foundation, in part by the NCCR program MaNEP, the EU Project CoMePhS, the SCOPES Grant No. IB7420-110784, and the K. Alex Müller Foundation.

[1] C. C. Tsuei *et al.*, Phys. Rev. Lett. **73**, 593 (1994).

[2] G. Deutscher, Rev. Mod. Phys. **77**, 109 (2005).

- [3] K. A. Müller, Nature (London) **377**, 133 (1995); J. Phys. Soc. Jpn. **65**, 3090 (1996).
- [4] K. A. Müller and H. Keller, *High- $T_c$  Superconductivity 1996: Ten Years after Discovery* (Kluwer Academic, Dordrecht, 1997), p. 7.
- [5] G. Binnig, A. Baratoff, H. E. Hoenig, and J. G. Bednorz, Phys. Rev. Lett. **45**, 1352 (1980).
- [6] H. Suhl, B. T. Matthias, and L. R. Walker, Phys. Rev. Lett. **3**, 552 (1959).
- [7] A. Bussmann-Holder, R. Micnas, and A. R. Bishop, Eur. Phys. J. B **37**, 345 (2003).
- [8] Amy Y. Liu, I. I. Mazin, and J. Kortus, Phys. Rev. Lett. **87**, 087005 (2001).
- [9] V. Z. Kresin and S. A. Wolf, Phys. Rev. B **46**, 6458 (1992).
- [10] J. E. Sonier, J. H. Brewer, and R. F. Kiefl, Rev. Mod. Phys. **72**, 769 (2000).
- [11] S. Serventi *et al.*, Phys. Rev. Lett. **93**, 217003 (2004).
- [12] A. Carrington and F. Manzano, Physica (Amsterdam) **385C**, 205 (2003).
- [13] T. Nakano, N. Momono, M. Oda, and M. Ido, J. Phys. Soc. Jpn. **67**, 2622 (1998).
- [14] R. Gilardi *et al.*, Phys. Rev. Lett. **88**, 217003 (2002).
- [15] E. H. Brandt, Phys. Rev. B **37**, R2349 (1988).
- [16] R. Khasanov *et al.*, Phys. Rev. B **72**, 104504 (2005).
- [17] T. Xiang and J. M. Wheatley, Phys. Rev. Lett. **76**, 134 (1996).
- [18] Ch. Niedermayer *et al.*, Phys. Rev. B **65**, 094512 (2002).
- [19] M.-S. Kim *et al.*, Phys. Rev. B **66**, 064511 (2002).
- [20] B. Mühlischlegel, Z. Phys. **155**, 313 (1959).
- [21] M. Oda, N. Momono, and M. Ido, Supercond. Sci. Technol. **13**, R139 (2000).
- [22] A. J. Drew *et al.*, Physica (Amsterdam) **374–375B**, 203 (2006).
- [23] R. Cubitt *et al.*, Phys. Rev. Lett. **91**, 047002 (2003).
- [24] R. S. Gonnelli *et al.*, Phys. Rev. Lett. **89**, 247004 (2002).
- [25] R. Stern *et al.*, Phys. Rev. B **51**, 15 478 (1995).
- [26] A. Furrer, *Superconductivity in Complex Systems* (Springer-Verlag, Berlin, 2005), p. 171.
- [27] D. R. Harshman *et al.*, Phys. Rev. B **69**, 174505 (2004).
- [28] C. Panagopoulos, J. L. Tallon, and T. Xiang, Phys. Rev. B **59**, R6635 (1999).
- [29] G. M. Luke *et al.*, Physica (Amsterdam) **282–287C**, 1465 (1997).
- [30] J. A. Skinta, T. R. Lemberger, T. Greibe, and M. Naito, Phys. Rev. Lett. **88**, 207003 (2002).
- [31] E. H. Brandt, J. Low Temp. Phys. **73**, 355 (1988).
- [32] J. K. Perry, J. Tahir-Kheli, and W. A. Goddard, Phys. Rev. B **65**, 144501 (2002).
- [33] E. S. Božin and S. J. L. Billinge, Phys. Rev. B **72**, 174427 (2005).
- [34] A. Damascelli, Z. Hussain, and Z.-X. Shen, Rev. Mod. Phys. **75**, 473 (2003).
- [35] T. Xiang, C. Panagopoulos, and J. R. Cooper, Int. J. Mod. Phys. B **12**, 1007 (1998).
- [36] K. Tamasaku, T. Ito, H. Takagi, and S. Uchida, Phys. Rev. Lett. **72**, 3088 (1994).
- [37] J. Hofer *et al.*, Phys. Rev. B **62**, 631 (2000).
- [38] N. E. Hussey *et al.*, Nature (London) **425**, 814 (2003).
- [39] S. Sahrakorpi, M. Lindroos, R. S. Markiewicz, and A. Bansil, Phys. Rev. Lett. **95**, 157601 (2005); R. S. Markiewicz *et al.*, Phys. Rev. B **72**, 054519 (2005).